



ELSEVIER

12 January 1998

PHYSICS LETTERS A

Physics Letters A 237 (1998) 297–306

# Motion of molecular motor ratcheted by internal fluctuations and protein friction

A. Mogilner<sup>a,1</sup>, M. Mangel<sup>b</sup>, R.J. Baskin<sup>c</sup>

<sup>a</sup> Department of Mathematics, University of California, Davis, CA 95616, USA

<sup>b</sup> Department of Environmental Studies, University of California, Santa Cruz, CA 95064, USA

<sup>c</sup> Section of Molecular and Cellular Biology, University of California, Davis, CA 95616, USA

Received 9 June 1997; revised manuscript received 9 October 1997; accepted for publication 14 October 1997

Communicated by C.R. Doering

## Abstract

We investigate theoretically a novel mechanism of transducing chemical energy into a directed force. A hypothetical motor protein is considered such that conformational changes induced by nucleotide binding and/or hydrolysis lead to asymmetric internal velocity fluctuations. We demonstrate that these fluctuations result in unidirectional motion if rectified by protein friction. The motor protein force–velocity relationship and other characteristics are computed based on analogy with known molecular motors. © 1998 Elsevier Science B.V.

PACS: 05.40; 82.20.M

Keywords: Brownian ratchet; Molecular motors; Protein friction

## 1. Introduction

Kinesin, myosin and RNA polymerase, moving along microtubules, actin filaments and DNA, respectively, are examples of biologically important families of molecular motors. In each example, proteins move unidirectionally along the track (i.e. protein or nucleic acid) [1–4]. The central question concerning these motor proteins is to characterize the mechanochemical transduction mechanism that generates a directed force and results in motor movement. Thermal ratchet models of molecular motors are based on rectifying Brownian diffusion by either periodic potentials asymmetric in space (which can be generated by periodic array of dipoles) or by a force with a zero mean

value asymmetric in time [5–7]. Power stroke models ascribe the motion of the motor to the conformational change in the motor induced by nucleotide binding and/or hydrolysis or to binding to the track [8,9]. Current models usually combine some features of both of these mechanisms [10,11].

In all such models the existence of an effective potential, periodic in space, in which the motors move, is necessary. Such potential, if asymmetric, rectifies stochastic motion and causes unidirectional propulsion. Atoms creating such a potential profile constantly fluctuate, causing dynamic changes of the potential shape. Then, in order for a model to be plausible, small changes in the potential shape must not lead to significant changes in the behavior of the motor. Some of the existing models do not have this feature. Besides the plausibility, from a purely theoretical point of view, it

<sup>1</sup> Corresponding author. E-mail: mogilner@math.ucdavis.edu.

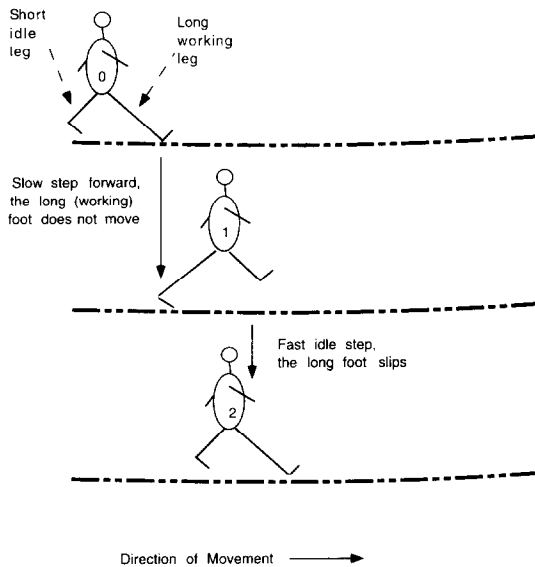


Fig. 1. The cycle of the “walk with a limp”. During a slow step forward the long working foot stays on the floor, and the body moves forward. During a fast idle step the long leg slips, and the body does not move.

would be interesting to find a heuristic mechanism of directed molecular motion not requiring any effective potential. Here we describe a novel (we are not aware of any other such model) mechanism having this feature.

This goal can be achieved if we first understand the following way of considering a one-legged man walking on a slippery floor. Let us consider a macroscopic “walker with a limp” having one “leg” slightly shorter than another (Fig. 1). We will denote the position of the longer leg ahead as “idle” ( $I$ ), and that with the longer leg behind as “forward” ( $F$ ). We will consider the transitions  $F \rightarrow I$  and  $I \rightarrow F$  as the “idle step” and “step forward”, respectively. We assume that because of the “limp” the idle step is quick, and the step forward is slow. Let us assume, first, that the walk takes place at slow rates in highly viscous liquid, at very low Reynolds numbers. Then, as explained in Ref. [12], the center-of-mass of the walker will not move. This conclusion depends drastically on two assumptions: (i) inertial forces can be neglected, and (ii) the friction is linear, i.e. the viscous resistance force is linearly proportional to the velocity.

Let us consider now a more difficult case when the walker moves on the floor, and the viscous resistance

is negligible in comparison with dry (sliding) friction between the longer foot and the track. Furthermore, let us assume that only the longer leg interacts with the track (the shorter one is just swinging in the air and needed as a “counterweight”), and that assumption (i) is valid (the inertial forces can be neglected). Now, when assumption (ii) is not valid (the dry friction is not linear), the effective unidirectional motion forward can occur. Indeed, if during relatively quick idle steps, the force between the legs exceeds the static friction, the longer leg slips, and the idle step would not lead to the motion of the walker’s center-of-mass. The following step forward, if slow enough (the force between the legs does not exceed the static friction), would not disrupt the cohesion between the longer foot and the floor, and then the center-of-mass of the walker would move the distance between the “feet” forward. The repetition of this cycle is equivalent to the effective unidirectional motion that is due to the left-to-right/right-to-left asymmetry of the speed of oscillations and friction non-linearity.

We will demonstrate in this Letter how a microscopic power stroke model vaguely similar to the described imaginary walk can explain qualitatively the unidirectional motion of the heuristic motor protein without postulating an effective periodic potential. Moreover, it will be shown that at model parameters analogous to those of some known molecular motors, the heuristic protein displays behavior quantitatively similar to the one experimentally observed. We will discuss biological implications of these conclusions in the last section. Here we want to stress that regardless of these conclusions the suggested mechanism is not a model of existing, known molecular motors (most notably kinesin in which the “two-legged walking” cycle may be confused with the imaginary walk described above).

## 2. Protein friction

From the description of the imaginary walker above it is clear that the source of some non-linear friction has to be introduced on the molecular scale to achieve a unidirectional motion driven by internal fluctuations at low Reynolds numbers. We suggest that protein friction caused by weak-binding interactions between a “motor” protein and “track” protein can play the role

of such force. The protein friction was introduced by Tawada and Sekimoto [13] (see also Ref. [11]) to explain the fact that the motion of elastic dynein heads associated with a rigid microtubule was much slower than that expected from dynein heads undergoing unrestricted Brownian motion. In this section we will derive the force–velocity relation for the protein friction originally obtained in Refs. [11,13].

Let us assume that the motor protein is sliding with the constant velocity,  $v$ , along the track protein and postulate that the “head” of the motor alternates between an attached state in which it is weakly bound to the track and a detached state. We introduce the average times the protein spends in the bound state,  $t_d$ , and in the detached state,  $t_a$ . (Parameters  $t_d$  and  $t_a$  are the inverted rates of detachment and attachment, respectively  $k_d = t_d^{-1}$ ,  $k_a = t_a^{-1}$ .) We assume that the bounds between the protein and track are elastic and obey Hooke’s law with the effective linear spring coefficient  $k_b$ , and that the elastic energy stored in the deformed spring is dissipated if the motor protein dissociates from the track spontaneously.

The effective average protein friction force,  $F_p$ , resisting the motion of the motor can be estimated as the associated rate of energy dissipation,  $W$ , divided by the average speed,  $v$ . Furthermore, the rate of energy dissipation can be computed as the average elastic energy lost after single detachment times the average frequency of detachments. If at the moment of attachment the bond between the motor and track is not overstretched, and the detachment occurs after time  $t_d$ , then the bound will be stretched on the distance  $t_d v$ , and the energy lost in the detachment  $w = k_b(t_d v)^2/2$ . The frequency of detachments,  $f_d$ , can be found as the fraction of time the protein is bound,  $t_d/(t_d + t_a)$  multiplied by the rate of detachment,  $k_d$ :  $f_d = k_d t_d/(t_d + t_a) = (t_d + t_a)^{-1}$ . Thus,

$$F_p = \frac{W}{v} = \frac{k_b}{2} \frac{t_d^2}{t_d + t_a} v, \quad \zeta_p = \frac{k_b}{2} \frac{t_d^2}{t_d + t_a}, \quad (1)$$

where  $\zeta_p$  is the protein friction drag coefficient.

In this derivation we neglected the viscous resistance to the motor’s motion from the solvent, which is justified if the effective protein friction drag coefficient is much greater than the corresponding viscous friction drag coefficient,  $\zeta_v \sim 6\pi\eta r$  (see also Ref. [13]). Here we assume that the viscous friction drag coefficient can be estimated roughly with Stokes’s for-

mula;  $\eta$  is the viscosity of water, and  $r$  is the size of the motor protein head. It will be shown below that for reasonable choice of parameters the inequality  $\zeta_p \gg \zeta_v$  is valid.

The fundamental difference between the protein friction and the viscous friction is that the latter is linear, while the former is not, despite the formal appearance of Eq. (1). This equation is valid under the condition that the time scale associated with protein motion is much longer than that associated with processes leading to the protein friction. On the other hand, if the time scale associated with protein motion is much shorter than that associated with processes leading to the protein friction, the protein–track bond does not have time to develop, and the protein friction can be neglected in comparison with the viscous friction.

This non-viscous, non-linear character of protein friction is the key factor in the mechanism of directed molecular motion. In the low Reynolds numbers limit (which is valid in molecular biological applications) the internal cyclic motion does not lead to unidirectional motion in the viscous liquid [12]. The necessary rectifying mechanism can be provided by the viscoelastic binding of the molecular motor to the track. In the next section we demonstrate how protein friction can rectify, unidirectionally, the internal velocity fluctuations.

### 3. Description of the model

We assume that the hypothetic motor protein consists of two globular domains (Fig. 2), which by analogy with two-headed motors (e.g. kinesin) we will call “heads”, and a flexible domain, which we will call the “spring”. One of the heads (“working head”, the analog of the longer leg of the imaginary walker) will be assumed to interact with the track in the way described in the previous section, while another one (“idle head”, the analog of the shorter leg) and the spring do not interact with the track. We will agree that the head interacting with the track is at the left, thus introducing left-to-right/right-to-left asymmetry without loss of generality. The realistic assumption which can explain why the hypothetic motor does not fall off the track is that either (i) there is a topological constraint of the motor having a “groove” inside

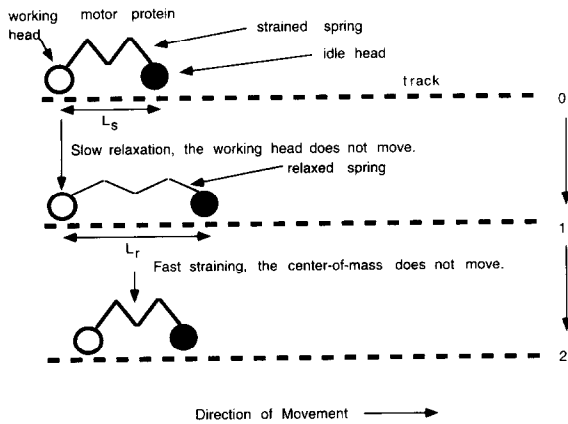


Fig. 2. The mechanochemical cycle of the motor protein. During slow spring relaxation the motion of the working head is stopped by the protein friction. At the same time, the idle head not interacting with the track and resisted by much smaller viscous friction moves to the right. Next, when an act of hydrolysis takes place, the spring contraction occurs so fast that there is no protein friction, and the heads converge symmetrically to the motor's center-of-mass. Repeated, this cycle causes the unidirectional motion.

which the track protein passes through the motor protein (analogously to RNA polymerase and DNA), or (ii) many such motors are connected loosely into a bundle and interact with a single-track protein (analogously to muscle myosin and actin).

We consider the spring existing in two states: strained ( $S$ ) and relaxed ( $R$ ). The spring in states  $S$  and  $R$  is characterized by the rest lengths  $L_s$  and  $L_r$  and by the effective elastic coefficients  $k_s$  and  $k_r$ , respectively. The spring in the strained state is shorter and stiffer:  $L_s < L_r$ ,  $k_s > k_r$ . We assume that the power stroke conformational transition  $R \rightarrow S$  involves ATP hydrolysis which takes place with the rate  $g_h$ . The relaxation conformational transition  $S \rightarrow R$  happens spontaneously with the rate  $g_r$ . Hydrolysis can not take place in the strained state.

We can now describe the mechanochemical cycle of the motor protein as follows (Fig. 2). We start from the state  $S$  where the spring assumes its rest length  $L_s$ . The next event is the slow, spontaneous relaxation of the spring, which is analogous to the slow step forward of the macroscopic imaginary walker. When this happens, the spring becomes less stiff, but its rest length is increased, so initially, there is some weak internal force stretching the spring. This force moves the working head to the left and the idle head to the

right. Because the internal force is weak, the motion is slow, the adhesion of the working head to the track is firm, and the protein friction resisting the motion of the working head is much greater than the viscous friction resisting the motion of the idle head. As a result, the working head is almost intact, while the idle head slowly shifts a distance  $L = L_r - L_s$  to the right.

Next, ATP is bound and/or hydrolyzed. Once this event occurs, the spring gets stiffer, its rest length is decreased, and the internal force contracts the spring. Because of the stiffer spring, this force may be great enough to contract the spring at such a speed that the contraction is completed in less time than the time associated with processes leading to the protein friction, and the working head "slips". Then, the motion of both heads is resisted by the viscous forces of the same magnitude, assuming a geometric left–right symmetry of the motor protein, and due to this symmetry this "fast idle step" leads to the working head's shift forward and the idle head's shift backward, respectively, both on the distance  $(L_r - L_s)/2$ . This ends the cycle; as a result the motor is in its initial state  $S$  again, and its center-of-mass is shifted to the right by about the distance  $(L_r - L_s)/2$ .

If the rates of hydrolysis and relaxation are  $g_h$  and  $g_r$ , respectively, then, the average velocity,  $V$ , of the motor can be computed as the average step per cycle multiplied by the cycle's rate,

$$V = \frac{g_r g_h}{g_r + g_h} \frac{L_r - L_s}{2}.$$

If a relatively small load force  $f$  is applied to the motor, then, to a first approximation, the protein would slow its drift (because of protein friction) by the speed  $f/\zeta_p$ , and the predicted force–velocity relation for the motor has the form

$$V = \frac{g_r g_h}{2(g_r + g_h)} (L_r - L_s) - \frac{f}{\zeta_p}. \quad (2)$$

## 4. Analysis of the model

### 4.1. Model parameters

In the order for the suggested mechanism to be of interest in molecular biological applications, the model parameters have to be chosen that (i) these parameters are of the same order of magnitude as those for

Table 1

Symbol	Dimensional value	Dimensionless value	Meaning
$g_h$	$\sim 10^3 \text{ s}^{-1}$	$\sim 0.1$	rate of hydrolysis
$g_r$	$10^3 \text{ s}^{-1}$	0.1	relaxation rate
$k_r$	0.01 pN/nm	0.04	effective spring coefficient in the relaxed state
$k_s$	0.5 pN/nm	2	effective spring coefficient in the strained state
$k_b$	20 pN/nm	80	effective spring coefficient of the bond between the motor protein and the track
$L_r$	40 nm	10	rest length of the effective spring in the relaxed state
$L_s$	20 nm	5	rest length of the effective spring in the strained state
$t_d$	$10^{-5} \text{ s}$	0.1	time in attached state
$t_a$	$10^{-5} \text{ s}$	0.1	time in detached state
$r$	50 nm	12.5	size of the protein's head
$k_B T$	$\simeq 4.1 \text{ pN nm}$	$\simeq 1$	thermal energy
$Q$	$\simeq 25 k_B T \simeq 100 \text{ pN nm}$	$\simeq 25$	free energy of hydrolysis
$\eta$	$10^{-9} \text{ pN s/nm}^2$	$1.6 \times 10^{-4}$	viscosity of water
$f$	$\sim \pm 1 \text{ pN}$	$\sim \pm 1$	load force
$\zeta_v$	$10^{-6} \text{ pN s/nm}$	0.04	viscous friction drag coefficient
$\zeta_p$	$5 \times 10^{-5} \text{ pN s/nm}$	2	protein friction drag coefficient

the known motors, such as myosin, kinesin and RNA polymerase, and (ii) the temporal, spatial and energetic scales have to conform with the model conditions and assumptions. Here we demonstrate that the model parameters given in Table 1 satisfy these requirements:

(i) We choose the size of the heads of the hypothetical motor  $r = 50 \text{ nm}$  (slightly greater than that for the known motors [1–3]), and the rest lengths of the spring  $L_s = 20 \text{ nm}$  and  $L_r = 40 \text{ nm}$ , of the same order of magnitude. Further, we take the effective spring coefficient in the strained state  $k_s = -0.5 \text{ pN/nm}$ , the same order of magnitude as the estimated stiffness of the effective spring in kinesin [9]. We assume that in the relaxed state the spring is very flexible, and  $k_r = 0.01 \text{ pN/nm}$ .

The free energy released from an ATP hydrolysis is  $Q \simeq 100 \text{ pN nm}$ . The minimal energy needed by the mechanochemical cycle described above  $E = (k_r + k_s)(L_r - L_s)^2/2$  is from ATP hydrolysis, and with our choice of the parameters the approximate equality  $E \simeq Q$  is satisfied.

(ii) We choose the stiffness of the bond  $k_b = 20 \text{ pN/nm}$ , comparable to that of hydrogen bonds, and the times of attachment and detachment  $t_a = t_d = 10^{-5} \text{ s}$ , comparable to that of myosin [1]. Then, from formula (1) we compute  $\zeta_p = 5 \times 10^{-5} \text{ pN s/nm}$ . From the Stokes's formula we estimate the viscous friction drag coefficient  $\zeta_p = 10^{-6} \text{ pN s/nm}$ , and the

inequality  $\zeta_p \gg \zeta_v$  is valid.

(iii) The characteristic time of the contraction phase can be estimated as the time of the spring relaxation  $T_s \sim \zeta_v/k_s = 2 \times 10^{-6} \text{ rms} \ll t_a, t_d$ . Thus, the protein friction can be neglected during the contraction phase of the cycle.

(iv) During spring relaxation, the biased drift of the idle head can be neglected in comparison with its diffusion (with effective diffusion coefficient  $D_v = k_B T/\zeta_v$ , where  $k_B T$  is the thermal energy), because the spring is very loose. The corresponding relaxation time scale can be estimated as  $T_r \sim (L_r - L_s)^2 \zeta_v/k_B T = 10^{-4} \text{ s} \gg t_a, t_d$ .

(v) We choose the rate of hydrolysis similarly to the known rates for kinesin and myosin, to be  $g_h \sim 10^3 \text{ s}^{-1}$ , and equal relaxation rate  $g_r \sim 10^3 \text{ s}^{-1}$ . These rates are an order of magnitude slower than the rate of spring relaxation, so the motor's mechanochemical cycle can be completed.

#### 4.2. Dimensional analysis

The conventional unit of force on the molecular scale is  $\bar{F} = 1 \text{ pN}$ . Also, it is convenient to measure distances in nm and have the thermal energy  $k_B T \simeq 4.1 \text{ pN nm}$  comparable to one, so we use the unit of length  $\bar{L} = 4 \text{ nm}$ . We choose the unit of time to be equal to the time scale of the spring relaxation:  $\bar{T} =$

$T_r = 10^{-4}$  s. Using these units we non-dimensionalized the model parameters. The corresponding dimensionless values are listed in Table 1.

### 4.3. Numerical studies

The dynamics of the working and idle heads are described with the following system of the Langevin-type equations:

$$\zeta_p \frac{dx}{dt} = -f + k \frac{y - x - L}{2} + N_x(t), \quad (3)$$

$$\zeta_v \frac{dy}{dt} = -k \frac{y - x - L}{2} + N_y(t). \quad (4)$$

Here  $x(t)$  and  $y(t)$  are the coordinates of the working and idle heads, respectively. The terms  $N_{x,y}(t)$  are modeled in the usual way as Gaussian white noises with the properties [14]

$$\langle N_{x,y}(t) \rangle = 0,$$

$$\langle N_{x,y}(t), N_{x,y}(t') \rangle = 2k_B T \zeta_{p,v} \delta(t - t').$$

The parameter  $f$  is the external load force which we consider applied to the working head.

The pair of variables  $(k(t), L(t))$  is the two-state continuous time Markov process: in the strained state  $(k(t), L(t)) = (k_s, L_s)$ , and in the relaxed state  $(k(t), L(t)) = (k_r, L_r)$ . The transitions  $(k_s, L_s) \rightarrow (k_r, L_r)$  and  $(k_r, L_r) \rightarrow (k_s, L_s)$  occur with the rates  $g_r$  and  $g_h$ , respectively.

The initial conditions used were  $x = 0$ ,  $y = L_s$ ,  $(k(t), L(t)) = (k_r, L_r)$ . To avoid time-consuming calculations with the time step less than the contraction phase time scale, we substituted the detailed description of the contraction phase with the following stochastic process. If at time  $t_n$  the transition  $R \rightarrow S$  takes place, then the center-of-mass of the motor does not move, while the distance between the heads abruptly changes to  $L_s$ :  $x_{n+1} = (x_n + y_n - L_s)/2$ ,  $y_{n+1} = (x_n + y_n + L_s)/2$ .

Eqs. (3), (4) in the non-dimensionalized form were integrated using Euler's method and the standard numerical procedure for taking into account the additive white noise terms [14]. The time step used was  $10^{-6}$  s (0.01 time unit). This time step provides a good qualitative description of the system and avoids instabilities.

## 5. Results

The numerical solution of Eqs. (3), (4) is shown in Fig. 3 for the case of absence of the external load. The displacement of the working head (in nm) is shown by the lower curve. The upper curve illustrates the displacement of the idle head. On the horizontal line below, (vertical) upward marks illustrate  $R \rightarrow S$  transitions while downward marks correspond to  $S \rightarrow R$  transitions. The calculations were for  $5 \times 10^{-3}$  s. It can be seen that when events of hydrolysis occur at  $\simeq 5 \times 10^{-4}$  s and  $3.7 \times 10^{-3}$  s, the working head jumps to the right, while the idle head jumps the same distance to the left. While the spring is strained and stiff, the amplitude of the idle head fluctuations is low. When the spring spontaneously relaxes, the average position of the working head does not move visibly, and the idle head's average position shifts to the right. While the spring is relaxed and very flexible, the amplitude of the idle head fluctuations is great.

The sample trajectory of the working head of the motor is shown in Fig. 4A. The mean displacement of the working head together with the expected standard deviation are plotted in Fig. 4B.

The average velocity of the motor was computed for different values of load force and rate of hydrolysis. The resulting force-velocity relation (Fig. 5) is almost linear, similar to experimental and theoretical results for kinesin motors [9,10,15–17]. For the values of parameters chosen, the free average velocity is of the order of 4000 nm/s ( $5 \mu\text{m/s}$ ), and the stall force is of the order of 0.25 pN. Such a value of the velocity is characteristic of myosin and greater than that of kinesin [4,15]. The value of the stall force is 1–2 orders of magnitude less than that of the known motors. The computed velocity is 15–20% smaller than that given by the analytical result (2). The source of this difference is the variance in the periods of time from relaxation to hydrolysis. Generally, when this time is equal or greater than the relaxation time, then the average step of the motor is equal to  $(L_r - L_s)/2$ . On the other hand, if this time is less than the relaxation time, the spring does not have time to relax before another act of hydrolysis occurs, which effectively decreases the average step of the motor.

The dependence of the motor velocity on the ATP hydrolysis rate in our model is shown in Fig. 6. The velocity grows at slow hydrolysis rates, when the re-

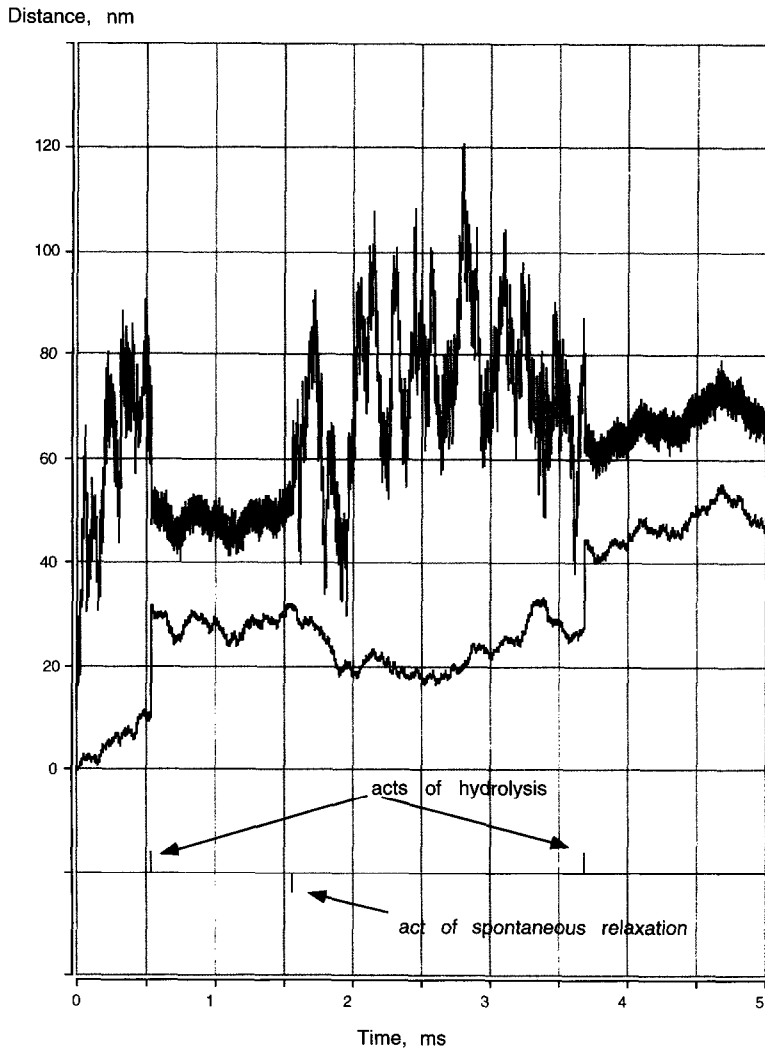


Fig. 3. The numerical run of the model (3), (4). The values of the model parameters are given in Table 1;  $g_h = 10^3 \text{ s}^{-1}$ ,  $f = 0$ . The upper and lower trajectories correspond to the displacements of the idle and working heads, respectively. On the horizontal line below, tiny vertical upward marks illustrate  $R \rightarrow S$  transitions, while downward marks correspond to  $S \rightarrow R$  transitions.

laxation time is shorter than the duration of the cycle. The velocity decreases at greater rates when the duration of the motor mechanical cycle becomes the rate-limiting factor, and frequent acts of hydrolysis effectively diminish the motor's step.

## 6. Conclusions and discussion

The suggested mechanism of motility is based on the following assumptions: (i) ATP hydrolysis sup-

plies the energy and regulates the asymmetric internal protein velocity fluctuations caused by the cyclic protein conformational changes, and (ii) protein friction rectifies these fluctuations.

This novel mechanism does not depend on an effective potential and has an interesting feature of being a velocity ratchet as compared to the usual positional ratchet models relying on the existence of the asymmetric periodic potential. The internal velocity fluctuations are not just thermal Brownian fluctuations, in which case the direction of velocity would

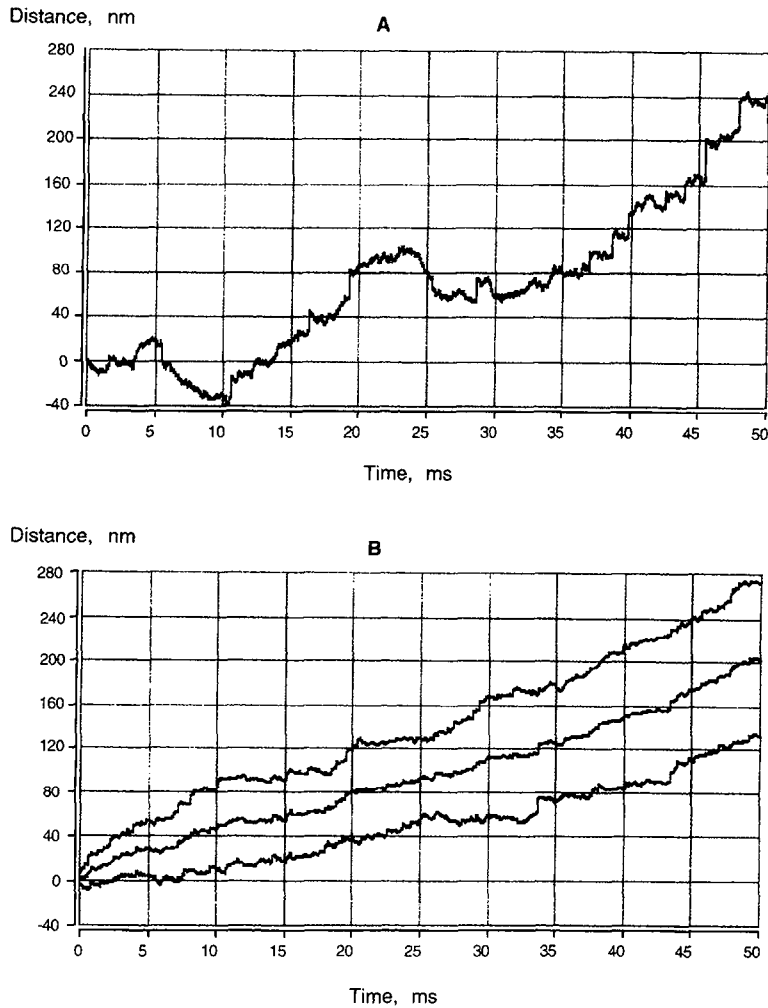


Fig. 4. (A) The sample trajectory of the working head interacting with the track computed numerically (for a period of  $5 \times 10^{-2}$  s) using the values of the model parameters given in Table 1;  $g_h = 1000 \text{ s}^{-1}$ ,  $f = 0$ . (B) The mean displacement and displacement variance, averaged over 25 separate runs, are shown. Data are plotted as mean  $\pm$  expected standard deviation.

be changing too often (approximately every  $10^{-18}$  s) for any reasonable rectifying mechanism to be viable. Instead, these fluctuations are regulated by relatively slow stochastic cycles of hydrolysis/relaxation which allows the non-linear (with respect to velocity) protein friction to be an effective velocity ratchet.

Calculations using realistic model parameters give velocity and force-velocity relations similar to those of known molecular motors, and stall force less than that of the known motors. We also calculated the energetic efficiency of the motor as the ratio of the work against friction forces during forward motion to the

energy of ATP consumed. At different model parameters the efficiency varies between 3% and 6%, which makes this motor apparently less efficient than known molecular motors. This low efficiency is due to alternating forward and backward steps of the motor, and the uncorrelated binding and conformational transitions mentioned above. The numerical computations demonstrated (see Fig. 4) that the mean variance of the protein displacement is a linear function of time, and that the motor is not a Poissonic stepper [18] (not shown). The fluctuations in displacement of the motor derive both from randomness in the step interval,



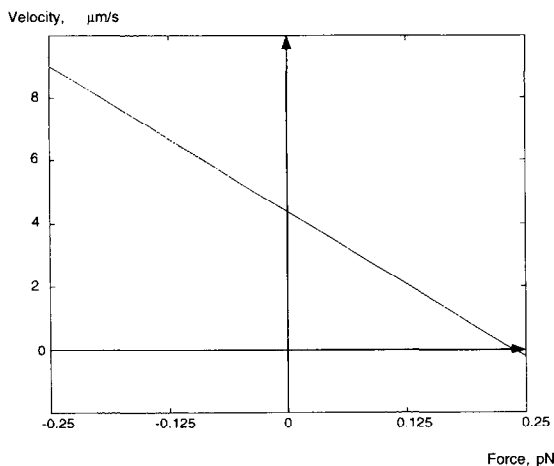


Fig. 5. The approximate force-velocity relation obtained from computing numerically the working head displacements for a period of  $10^{-1}$  s, and averaging over 25 separate runs. The values of the model parameters given in Table 1 were used;  $g_h = 10^3 \text{ s}^{-1}$ . The velocity was computed at the values of the load force from  $-0.25 \text{ pN}$  to  $0.25 \text{ pN}$  with an increment of  $\frac{1}{16} \text{ pN}$ , and then the linear fit was obtained (the deviations of data from the linear fit are very small).

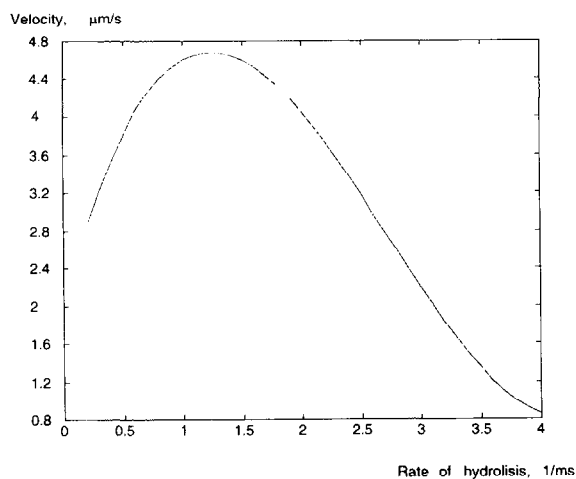


Fig. 6. The approximate dependence of the motor's average velocity on the ATP hydrolysis rate computed numerically using the values of the model parameters given in Table 1;  $f = 0$ . The velocity was computed at the values of the hydrolysis rate from  $0.2 \times 10^3 \text{ s}^{-1}$  to  $4 \times 10^3 \text{ s}^{-1}$  with an increment of  $0.2 \times 10^3 \text{ s}^{-1}$  and then the polynomial fit was obtained.

and irregularities in the step size.

Our postulated motor may be a primitive version of existing (linear) molecular motors. The actions of myosin and kinesin also depend on ATP hydrolysis and protein conformational changes; however, this ac-

tion is more highly regulated. In these motors, binding to the track proteins, unlike in our model, is presumably correlated with conformational transitions. There is not enough information known on the dynein-tubulin interaction to compare with the present model. The force-velocity relation for RNA polymerase behaves differently from the linear decrease.

Because of these reasons the suggested mechanism may not explain the action of known molecular motors, Nevertheless, this model can be relevant to some aspects of the behavior of motor proteins moving along track proteins. For example, perhaps the inchworming mode of the RNA polymerase propulsion can be explained with the protein friction coupled to internal elastic fluctuations [19]. Furthermore, the relevant mechanism works *in vivo* on a macroscopic level: gastropods move on surfaces generating muscular waves which are rectified by visco-elastic friction of pedal mucus covering the surface [20]. A "series elastic" component [21], clearly present in myosin motors, is an inherent and required part of our postulated motor. Perhaps elasticity is a required component of the myosin motor and is not incidental to its structure. Another interesting feature of this model is the requirement for two model heads, both to develop force, and one of them to be the source of the protein friction necessary to rectify movement. (Both heads are not required to be on the same motor molecule.)

## Acknowledgement

We would like to thank G. Oster for valuable discussions and suggestions.

## References

- [1] J. Spudlich, *Nature* 372 (1994) 515.
- [2] R. Vale, *Cell* 78 (1994) 733.
- [3] H. Yin, M.D. Wang, K. Svoboda, R. Landick, S.M. Block, J. Gelles, *Science* 270 (1995) 1653.
- [4] S. Block, *Trends in Cell. Biol.* 5 (1995) 169.
- [5] D. Astumian, M. Bier, *Phys. Lett.* 72 (1993) 1766.
- [6] N. Cordova, B. Ermentrout, G. Oster, *Proc. Natl. Acad. Sci. (USA)* 89 (1991) 339.
- [7] M.O. Magnasco, *Phys. Rev. Lett.* 72 (1993) 2656.
- [8] J. Prost, J.-F. Chauwin, L. Peliti, A. Ajdary, *Phys. Rev. Lett.* 74 (1994) 2652.
- [9] M. Derenyi, F. Vicsek, *Proc. Natl. Acad. Sci. (USA)* 93 (1996) 6775.

- [10] C. Peskin, G. Oster, *Biophys. J.* 68 (1995) 202.
- [11] S. Leibler, D. Huse, *J. Cell. Biol.* 121 (1993) 1357.
- [12] E. Purcell, *Amer. J. Physics.* 45 (1977) 3.
- [13] K. Tawada, K. Sekimoto, *J. Theor. Biol.* 150 (1991) 193.
- [14] C. Doering, *Modeling complex systems: stochastic processes, stochastic differential equations and Fokker-Planck equations*, in: *Lectures in Complex Systems* (Addison-Wesley, Redwood City, 1990).
- [15] T. Yanagida, A. Ishijima, *Biophys. J.* 68 (1995) 312.
- [16] J. Finer, R. Simmons, J. Spudlich, *Nature* 368 (1994) 113.
- [17] M. Jiang, M. Sheet, *Bioessays* 16 (1994) 531.
- [18] K. Svoboda, P. Mitra, S. Block, *Proc. Natl. Acad. Sci. (USA)* 91 (1994) 11782.
- [19] H-Y. Wang, T. Elston, A. Mogilner, G. Oster, *Biophys. J.*, in press.
- [20] M. Denny, *Nature* 285 (1980) 160.
- [21] A.F. Huxely, R.M. Simmons, *Nature* 233 (1971) 533.